Mon. Not. R. Astron. Soc. **353,** L29–L33 (2004) doi:10.1111/j.1365-2966.2004.08266.x

Discovery of high-amplitude X-ray variability in the Seyfert–LINER transition galaxy NGC 7589

W. Yuan,[1⋆] St. Komossa,[2] D. Xu,[3] J. P. Osborne,[4] M. G. Watson[4] and R. G. McMahon[1]

[1] *University of Cambridge, Institute of Astronomy, Madingley Road, Cambridge CB3 0HA*
[2] *Max-Planck Institut für Extraterrestriche Physik, Postfach 1312, 85741 Garching, Germany*
[3] *National Astronomical Observatories, Chinese Academy of Sciences, Beijing 100012, China*
[4] *Department of Physics and Astronomy, University of Leicester, Leicester LE1 7RH*

Accepted 2004 July 30. Received 2004 July 29; in original form 2004 June 14

ABSTRACT

We present the first result of a programme to search for large flux variations in the X-ray sources of the *XMM* Serendipitous Survey compared to previous *ROSAT* observations. An increase in X-ray flux by a factor >10 was discovered from the nucleus of the galaxy NGC 7589 on a time-scale of less than 5 yr. The 0.4–10 keV *XMM* spectrum can be approximated by a power law with photon index of 1.7–1.8, though it seems to flatten above 5 keV, suggesting a possible complex model, such as partial covering or disc reflection. A classification based on an analysis of its optical spectrum places NGC 7589 in the Seyfert region, but close to the Seyfert–LINER (low-ionization nuclear emission-line region) borderline on the active galactic nucleus (AGN) diagnostic diagrams. We classify NGC 7589 as either Seyfert 1.9 or LINER I, in the light of the detection of a broad Hα line, which makes NGC 7589 an AGN in the low-luminosity regime. We interpret the observed variability in terms of either changes in covering factor of absorbing gas in the AGN, or variability in the intrinsic X-ray luminosity. Should the latter be the case, the inferred Eddington accretion rate increased from the radiatively inefficient accretion-dominated regime to a value close to the putative critical value, at which a transition of the accretion mode is supposed to take place. This possibility presents a new prospect of studying accretion physics in the central black holes of external galaxies by direct observing changes of 'spectral state', as is common in stellar black hole binary systems.

Key words: galaxies: active – galaxies: individual: NGC 7589 – X-ray: galaxies.

1 INTRODUCTION

In contrast to typical active galactic nuclei (AGN), low-luminosity AGN (LLAGN) as a class radiate at a power much lower than the Eddington luminosity,[1] i.e. in terms of the bolometric/Eddington luminosity ratio (Eddington ratio), $L_{\rm bol}/L_{\rm Edd} < 0.01$ (Ho 2004). As such, black holes in LLAGN are hypothesized to accrete via radiatively inefficient accretion flows (RIAF; see Quataert 2001 for a review), such as an advection-dominated accretion flow (ADAF; see Narayan, Mahadevan & Quartaert 1998 for a review), rather than an optically thick, geometrically thin standard accretion disc (thin disc hereafter; Shakura & Sunyaev 1973). In fact, the high end of their $L_{\rm bol}/L_{\rm Edd}$ distribution encompasses the critical value[2] above which a RIAF is to be replaced with a standard thin disc. As a consequence, in LLAGN exhibiting violent variability of luminosity, a transition of the accretion mode is expected to take place once $L_{\rm bol}/L_{\rm Edd}$ crosses the critical value. This is where observations can be used to test black hole accretion theories. While such a transition of the accretion mode can, indeed, explain the observed changes of the 'spectral states' in X-ray binaries (e.g. Esin et al. 1997; Meyer, Liu & Meyer-Hofmeister 2000), the situation is not clear in massive extragalactic black hole systems. On galactic scales, the major difficulty in observations is the long time-scales of the X-ray variability, which is roughly scaled with the black hole mass. Timely detection of violent variability in AGN, especially in LLAGN, is of particular interest in this regard.

About 40 per cent of nearby galaxies exhibit LLAGN activity (Ho, Filippenko & Sargent 1997), the majority of which belong to a class known as low-ionization nuclear emission-line regions (LINER, Heckman 1980). Large-amplitude X-ray variability is sometimes seen in low-luminosity Seyferts (e.g. Nandra et al. 1997), whereas no similar behaviour is found in LINERs (e.g. Ptak et al. 1998; Komossa, Böhringer & Huchra 1999; Terashima et al. 2002).

⋆E-mail: wmy@ast.cam.ac.uk

[1] $L_{\rm Edd} = 1.26\,M_{\rm bh} \times 10^{38}$ erg s^{-1}, where $M_{\rm bh}$ is the black hole mass in $M_\odot$.

[2] Hypothesized as 0.01–0.1 times the Eddington ratio for ADAF (Narayan et al. 1998); however, observations show that the transition always occurs at a luminosity around 10^{37} erg s^{-1} (e.g. Tanaka 1999), which corresponds to a few per cent of the Eddington ratio.

Table 1. Summary of the *XMM* observations and data reduction.

orbit number	orbit 272	orbit 361	
detectors	MOS1/2	MOS1/2	PN
date	2001 June 3	2001 November 11	
observation ID	0066950301	0066950401	
duration (ks)	12.2	12.6	13.2
GTI CR[a]	0.35	0.35	1.0
events pattern	0–12	0–12	0–4
good exposure (s)	7366/7151	9175/9826	8133
net source CTS	555/503	243/276	843
src CR (10^{-2} count s^{-1})	$7.5/7.0 \pm 0.4$	$2.6/2.8 \pm 0.3$	10.4 ± 0.7

[a]Count-rate criteria for rejecting high-background periods identified by single events (PI > 10 000, pattern = 0) in units of count s^{-1}.

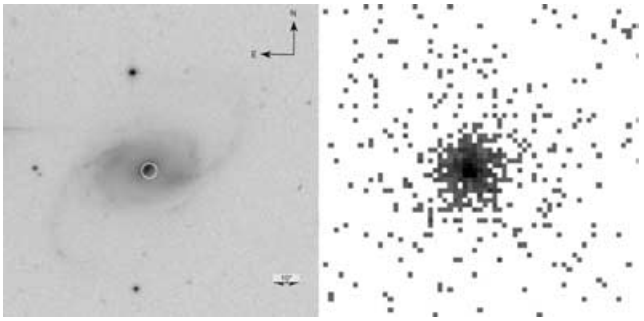

Figure 1. Optical r'-band (left) and X-ray (right; *XMM* MOS-1, orbit 272) images of NGC 7589 on the same scales. A circle on the optical image represents the position and its 3σ error of the X-ray source. A 10-arcsec angular distance corresponds to 5.65 kpc.

In this Letter, we report the discovery of large-amplitude X-ray variability in the galaxy NGC 7589 at a redshift of 0.0298. This is one of the first results of a search of long-term highly variable X-ray sources (Yuan et al. in preparation; see also Yuan et al. 2002) of the *XMM* Serendipitous Survey (Watson et al. 2001). We selected candidates which varied by a factor of at least 10 for further follow-up studies in the X-ray and other wavebands. We used a luminosity distance of 123.3 Mpc calculated from the radial velocity of 8562 km s^{-1} (LEDA[3]) relative to the cosmic microwave background by assuming $H_0 = 71$ km s^{-1} Mpc^{-1}, $\Omega_\Lambda = 0.73$ and $\Omega_m = 0.27$.

2 THE *XMM* X-RAY DATA OF NGC 7589

2.1 *XMM* observations

The *XMM* observations, data screening and source extraction are summarized in Table 1. It should be noted that the PN camera was not active during the first observation in the *XMM* orbit 272. The *XMM* SCIENCE ANALYSIS SYSTEM (SAS, v. 5.4) was used for data reduction. Source X-ray events were extracted from a circle of 32-arcsec radius. Background events were extracted from source-free regions using a concentric annulus of 40-/120-arcsec radii for the MOS detectors, and circles of 32-arcsec radius at the same CCD read-out column as the source position for the PN detector. In both observations, an X-ray source was detected at the position RA = $23^h18^m15\overset{s}{.}6$, Dec. = $0°15'38\overset{''}{.}9$ (J2000), coincident with the nucleus of NGC 7589 (Fig. 1). The source spatial profile in the 0.3–2keV band was found to be point-like. No time variability was found on time-scales shorter than the *XMM* observational intervals of about 12 ks. The galaxy was also observed with the *XMM* Optical Monitor (OM) with the UVW1 filter (2000–4000 Å) and was detected as an extended source.

[3] Data base for physics of galaxies (http:// Leda.univ-lyon1.fr).

2.2 The *XMM* X-ray spectra and fluxes

The MOS1 and MOS2 spectra were co-added to produce a single, combined spectrum. We used XSPEC (v.11.3) for spectral modelling. Spectral bins below 0.4 keV were excluded because of uncertain calibration below 0.35 keV (XMM-SOC-CAL-TN-0018). From orbit 361, we have both PN and MOS spectra; they were jointly fitted with independent normalizations. In comparisons of the two observations, the fitted spectral parameters agree with each other for most or all the parameters except the normalizations, which differ by a factor of $\simeq$2.5. To improve photon statistics, we also performed fits to the two spectra from the different epochs with most of the parameter values tied together. The results are summarized in Table 2 and explained below.

Table 2. Spectral fits to *XMM* data for NGC 7589.

data set	orbit 272	orbit 361	both orbits
detectors	MOS	MOS+PN	orb272/orb361
power law, fixed $N_H = N_H^{Gal} = 4.06 \times 10^{20}$ cm^{-2}			
Γ	1.69 ± 0.09	1.68 ± 0.08	1.68 ± 0.06
$N_{1keV}/10^{-5}$	14.2 ± 0.9	5.5 ± 0.5	$14.1 \pm 1.0/5.4 \pm 0.5$
χ^2/d.o.f.	44/39	58/62	103/102
partial covering by cold matter, $N_H = N_H^{Gal}$			
Γ	$1.80^{+0.07}_{-0.11}$	1.74 ± 0.10	$1.77^{+0.04}_{-0.08}$
$N_H/10^{22}$	30^{+85}_{-20}	48^{+68}_{-37}	40^{+62}_{-23}
covering factor	$0.54^{+0.35}_{-0.27}$	$0.54^{+0.46}_{-0.24}$	$0.55^{+0.25}_{-0.25}$
χ^2/d.o.f.	38/37	55/60	93/100
partial covering by ionized absorber (absori), $N_H = N_H^{Gal}$			
Γ	1.77 ± 0.14	1.73 ± 0.10	1.75 ± 0.08
$N_H/10^{22}$	70_{-56}	74_{-61}	76_{-30}
ξ	123^{+2755}_{-123}	31	$137^{+468}_{-137}/60^{+166}_{-60}$
covering factor	$0.54^{+0.26}_{-0.39}$	$0.55^{+0.28}_{-0.50}$	$0.53^{+0.17}_{-0.25}$
χ^2/d.o.f.	37/35	55/58	92/96
reflection from cold disc (pexrav), fixed $N_H = 4.06 \times 10^{20}$ cm^{-2}			
Γ	1.85 ± 0.14	$1.74^{+0.15}_{-0.06}$	1.79 ± 0.08
rel-refl	$8.0^{+4.6}_{-5.4}$	$3.5^{+5.0}_{-3.5}$	$5.9^{+4.8}_{-3.9}/5.0^{+4.9}_{-4.0}$
χ^2/d.o.f.	38/38	56/61	95/100
reflection from ionized disc (pexriv), fixed $N_H = N_H^{Gal}$			
Γ	1.77 ± 0.20	1.73 ± 0.13	$1.75^{+0.10}_{-0.08}$
ξ	157	3	$186^{+224}_{-186}/4^{+217}_{-4}$
rel-refl	$3.5^{+11.3}_{-2.9}$	$3.3^{+5.1}_{-3.3}$	$3.2^{+5.0}_{-2.4}$
χ^2/d.o.f.	37/37	56/60	94/99

Errors are at the 90 per cent level when quoted; if not given, they are not constrained within the physically meaningful ranges.
N_H: column density in units of cm^{-2}.
$N_{1\,keV}$: normalization at 1 keV in units of photon cm^{-2} s^{-1} keV^{-1}; values quoted are for the combined MOS detectors.
rel-refl: factor of reflection relative to the primary continuum.
ξ: ionization parameter defined as L/nR^2 for absorber with density n at a distance R to a source with an ionizing luminosity L (Done et al. 1992).

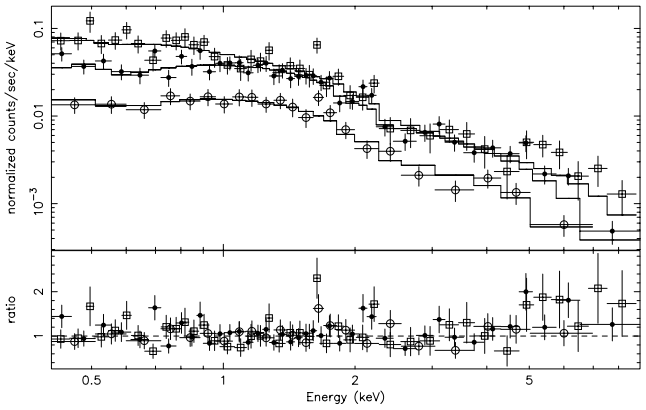

Figure 2. *XMM* spectral data, the model fit and the residual as data-to-model ratio. The model is for a joint power-law fit to the spectra of the combined MOS in orbit 272 (dots), and the MOS (circles) and the PN (squares) in orbit 361, in the restricted 0.4–2 keV band and extrapolated to higher energies. A spectral flattening can be seen for both orbits.

Power-law models. A simple absorbed power law gives statistically acceptable fits to all the spectra; however, the fitted $N_{\rm H}$ is lower than the H I column density along the line of sight $N_{\rm H}^{\rm Gal} = 4.06 \times 10^{20}\,{\rm cm}^{-2}$ (at the 92 per cent confidence level). The fits over the restricted 0.4–2 keV and 2–10 keV ranges yielded a photon index in the low-energy band $\Gamma_{\rm low-E} = 1.72 \pm 0.12$ and one in the high-energy band $\Gamma_{\rm high-E} = 1.42^{+0.20}_{-0.26}$, respectively, indicating a spectral flattening towards high energies. This can be seen from the residuals in Fig. 2, which compares the data to a fitted model using only the 0.4–2 keV spectra. In fact, a broken power-law model of $\Gamma_{\rm low-E} = 1.75^{+0.10}_{-0.16}$ and $\Gamma_{\rm high-E} = 1.03^{+0.40}_{-0.47}$ improved the fit significantly, with $\Delta\chi^2 = -10$ for two additional free parameters; the F-test gave a probability level for no improvement over the single power law fit as being <1 per cent. The fitted $N_{\rm H}$ was also recovered to value consistent with $N_{\rm H}^{\rm Gal}$.

Complex spectral models. Spectral flattening is often seen in AGN as a result of scattered X-rays, likely by an accretion disc, or by X-rays transmitted through optically thick gas. Accordingly, we fit disc-reflection and partial-covering models to the spectra. Both types of models, either cold or ionized, were found to provide excellent and statistically indistinguishable fits to all the data. The overall absorption $N_{\rm H}$ values were in general consistent with $N_{\rm H}^{\rm Gal}$. The disc inclination was not constrained and so was fixed at 30°. The disc-reflection models require a larger reflection/direct ratio (i.e. >2) than that from a medium subtending a 4π solid angle, implying that the primary continuum is partially obscured in this case. No significant iron Kα line was seen at around 6.4 keV; 90 per cent upper limits for the line equivalent width were found to be 550 and 110 eV for the first and second observations, respectively. Modelling the high-energy excess simply by an extremely broadened iron line (the *discline* model) gave no satisfactory fit.

X-ray fluxes and luminosities. The X-ray fluxes were calculated using the best-fitting power-law spectral model with $N_{\rm H} = N_{\rm H}^{\rm Gal}$, i.e. $\Gamma = 1.68\,(1.73)$ for 0.5–10 (0.5–3) keV. In the 0.5–10 keV band, the Galactic absorption corrected fluxes are 9.1×10^{-13} and $3.7 \times 10^{-13}\,{\rm erg\,cm^{-2}\,s^{-1}}$ for orbits 277 and 361, respectively, which correspond to luminosities of 1.7×10^{42} and $0.7 \times 10^{42}\,{\rm erg\,s^{-1}}$, respectively. In consideration of the likely presence of the partial-covering or disc-reflection (assuming a flat disc subtending a 2π solid angle) component, the intrinsic X-ray luminosities are likely to be a factor of $\sim$2 and 3–5 higher, respectively.

3 THE LONG-TERM X-RAY VARIABILITY

3.1 Fluxes from the *ROSAT* and *Einstein* data

NGC 7589 was within the field of view (10 arcmin off-axis) of a 5.4 ks pointing observation made by *ROSAT* with its Position Sensitive Proportional Counter (PSPC) detector (0.1–2.4 keV) on 1995 June 16–17. No source was detected at the position of NGC 7589. We derived a limit on the source flux in two ways. The first was a simple estimate using the count rate of the weakest detected source neighbouring NGC 7589. This led to a conservative upper limit on the source count rate of $2.7 \times 10^{-3}\,{\rm count\,s^{-1}}$. A more rigorous estimation was made using the PSPC X-ray image. Photon counts from the background and a possible source were extracted from a circle of 45-arcsec radius (enclosing 95 per cent of the power of the point spread function, hereafter PSF) at the position of NGC 7589, yielding a measured $C_{\rm s+b} = 17$ count. Following Poisson statistics, the expected counts $\bar{C}_{\rm s+b}$ is distributed as $\bar{C}_{\rm s+b} \leqslant 24\,(27)$ at the (one-tail) probability of 95 (99) per cent. The contribution of the background was estimated as $C_{\rm b} = 9.5$ count, using the averaged local background estimated from an annulus of 90-/225-arcsec radii. The expected net number of source counts was estimated to be $\bar{C}_{\rm s} \leqslant \bar{C}_{\rm s+b} - C_{\rm b} = 14.5\,(17.5)$ count. After correction for the vignetting and extraction aperture, the source count rate was estimated to be $\leqslant 2.9(3.4) \times 10^{-3}\,{\rm count\,s^{-1}}$. Assuming the spectrum to be the same as that measured with *XMM*, we derived the 0.1–2.4 keV flux limit to be 5.9 (7.0) $\times 10^{-14}\,{\rm erg\,cm^{-2}\,s^{-1}}$ at the 95 (99) per cent level, after correction for the Galactic absorption.

A less stringent flux limit of $5.6 \times 10^{-13}\,{\rm erg\,cm^{-2}\,s^{-1}}$ was set by the data extracted from the *ROSAT* All-Sky Survey performed in 1992. By searching the data archives of various X-ray satellites, we found that, in addition to *ROSAT*, NGC 7589 was also serendipitously observed by the *Einstein* Observatory with its Imaging Proportional Counter (IPC) detector at an off-axis angle of 10.8 arcmin for 2540 s in 1980 May. Similar estimation using a source extraction radius of 3 arcmin yielded a limit on the unabsorbed flux of $3.5 \times 10^{-13}\,{\rm erg\,cm^{-2}\,s^{-1}}$. Both limits are quoted at the 95 per cent level.

3.2 Variability in the X-rays and UV

For comparison of the fluxes among the different missions, we used the overlapping 0.5–2.4 keV energy band. The light curve in Fig. 3 reveals a dramatic increase in luminosity, by a factor of >10, occurring sometime between the *ROSAT* pointing and the *XMM* observation in orbit 272, on a time-scale $\lesssim$5 yr. Given the poor sampling, the flux seen by *XMM* may not represent the flux at the 'highest

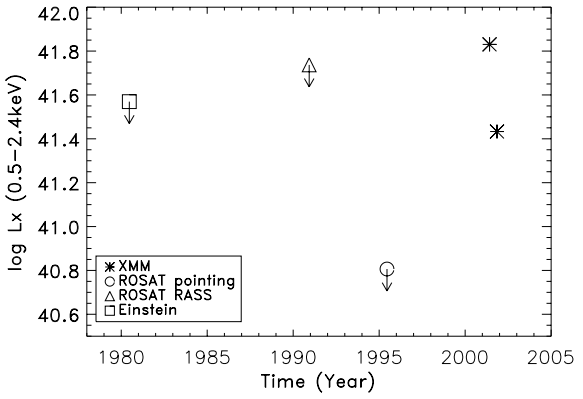

Figure 3. The long-term light curve of the 0.5–2.4 keV X-ray luminosity of NGC 7589. Upper limits are at the 95 per cent confidence level.

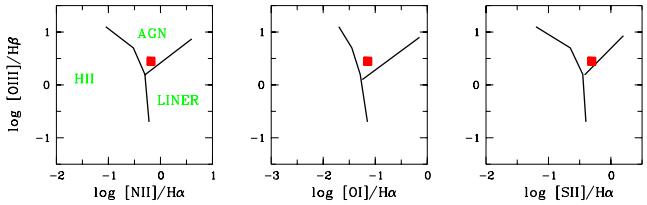

Figure 4. The position of NGC 7589 in the diagnostics diagrams, based on its optical emission-line ratios.

state', which means that the peak luminosity could be even higher. Therefore the actual variability amplitude must be >10. The flux decreased by a factor of 2.5 between the two *XMM* observations over a period of 5 months, whereas the overall 0.4–10 keV spectral shape appeared to remain unchanged.

The OM UV magnitude within a central 6-arcsec-radius aperture was measured to be 16.99 ± 0.06 and 17.03 ± 0.05 for orbits 272 and 361, respectively. However, the emission is dominated by the extended bulge and no significant point-like source is present; thus no meaningful constraint on variability could be obtained.

4 OPTICAL SPECTROSCOPIC CLASSIFICATION

NGC 7589 was observed spectroscopically in the Sloan Digital Sky Survey (SDSS; York et al. 2000) on 2000 September 29, about 8 months prior to the high state caught by *XMM*. The spectrum was taken from the SDSS Data Release 2. The contribution of stellar light from the host galaxy was subtracted from the observed spectrum by modelling stellar absorption lines employing a range of galaxy spectral templates, using the method developed by Li et al. (2004) (A full account of the spectral analysis and estimation of the black hole mass for NGC 7589 is to be presented elsewhere.) Single-component Gaussians were fit to the emission lines. This provided satisfactory fits, except for Hα which required the presence of a second, broad component. The broad Hα line, which was blueshifted, had a width of FWHM $\approx 3428\,\mathrm{km\,s^{-1}}$, compared with the narrow lines of FWHM $\approx 228\,\mathrm{km\,s^{-1}}$.

The emission-line ratios place NGC 7589 in the Seyfert region of the diagnostic diagrams of Veilleux & Osterbrock (1987), close to the borderline with the LINERs (see Fig. 4). The same conclusion also holds if we use the classical definition of LINERs (Heckman 1980) which only makes use of oxygen emission-line ratios. For LINERs, [O II]λ3727/[O III]λ5007 > 1 and [O I]λ6300/[O III]λ5007 > 1/3 (and lower for '[O I]-weak' LINERS), whereas NGC 7589 shows [O II]λ3727/[O III]5007$\lambda \approx$ 0.5 and [O I]λ6300/[O III]λ5007 = 0.1. This places NGC 7589 in a region populated by Seyferts (see fig. 1b of Filippenko & Terlevich 1992) but, again, close to the borderline with LINERs. We note that the measured line ratios are insensitive to the galaxy spectrum subtraction – the same result holds even when the unsubtracted spectrum is used. The detection of a broad component in Hα reveals a type I AGN and leads to the classification of NGC 7589 as either a Seyfert 1.9 or possibly a LINER I.

5 DISCUSSION

5.1 Classification of NGC 7589

On the classification diagrams based on emission-line ratios, the distribution of the LLAGN in the Ho (2004) sample has a continuous and smooth transition between Seyferts and LINERs. This makes the conventional, 'operational' dividing lines somewhat arbitrary and physically insignificant. NGC 7589 falls within the area in which galaxies are classified as Seyferts; however, it is too close to the border region to allow an ultimate classification as either a Seyfert or LINER. A similar conclusion holds when the emission-line width is considered (e.g. Ho, Filippenko & Sargent 2003). We therefore treat NGC 7589 as a member of the important 'borderline objects', which probe the physics in transition from Seyfert to LINER. Optically, NGC 7589 is a giant, bulge-dominated low-surface-brightness galaxy (Pickering et al. 1997).

The high-amplitude X-ray variability detected is exceptional, given the transition nature of NGC 7589. While there is a trend in Seyferts showing enhanced X-ray variability with decreasing luminosity (e.g. Nandra et al. 1997), the trend breaks at low luminosities; in particular, LINERs do not vary much in X-rays (e.g. Ptak et al. 1998; Komossa et al. 1999; Terashima et al. 2002). Those that do rarely exceed a variability of a factor of two. The high-amplitude variation in the X-ray luminosity of the order of magnitude of $10^{42}\,\mathrm{erg\,s^{-1}}$ on time-scales of a few years suggests black hole accretion as the ultimate source of the power in NGC 7589. This is in line with the AGN nature of NGC 7589 indicated by the broad $H\alpha$ line.

We may ask whether the *XMM* 'high state' or the *ROSAT* 'low state' is more representative of the average X-ray luminosity. We assume that the narrow-line luminosities in the SDSS spectrum represents the average state of NGC 7589. By making use of the $L_{\mathrm{H}\alpha} \sim L_{\mathrm{X}}$ correlation for LLAGN (Halderson et al. 2001), a luminosity of $L_{\mathrm{X}} \sim 1 \times 10^{41}\,\mathrm{erg\,s^{-1}}$ ($\sim 1.5 \times 10^{41}$) is predicted in the 0.1–2.4 keV (0.5–10 keV) band, assuming $\Gamma = 1.7$. This value is significantly below the high-state luminosity, and is comparable to the low-state upper limit. This suggests that probably NGC 7589 normally behaves like a LLAGN, and underwent an outburst that was caught by *XMM*. At the high state, L_{X} reached the lower end of the typical Seyfert luminosity range ($10^{42-44}\,\mathrm{erg\,s^{-1}}$), and the very upper end of the LINER range. The power-law model is again consistent with both Seyfert and LINER types, whereas the partial covering/reflection model would favour a Seyfert.

5.2 The X-ray variability

In general, X-ray variability in AGN may have two distinct origins: variations in intrinsic radiation and variations in absorption/obscuration. Below we discuss briefly our results in this context. For NGC 7589, the mass of the central black hole is of the order of $10^7\,\mathrm{M_\odot}$, as found in our ongoing follow-up work (Yuan et al. in preparation).

Variable absorption. Evidence for variable absorption has been found in some Seyfert galaxies, especially in Type 2 and intermediate-type, on time-scales of months to years (e.g. Risaliti, Elvis & Nicastro 2002) through variation of N_{H} and/or the covering factor (e.g. NGC 3227: Komossa et al. 2001, NGC 3516: Guainazzi, Marshall & Parmar 2001). The absorbers are postulated to be gas clouds in the 'broad-line region' (BLR) producing relatively fast variations, and a parsec-scale 'torus' producing relatively long-term variations. In particular, NGC 7589 might be an analogue to the LLAGN in M 51, in which a suspected large-amplitude X-ray variation could be well explained by placing a thick ($N_{\mathrm{H}} > 10^{24}$) absorber on and off the line of sight (Fukazawa et al. 2001).

For the *ROSAT* low state, taking the best-fitting *cold* partial covering model for the *XMM* spectrum at the highest state (Table 2) and increasing artificially the covering factor up to $\gtrsim$0.95, the soft X-ray

flux was then suppressed below the *ROSAT* detection limit. For the flux decrease between the two *XMM* observations, we considered the joint fit with the partial covering model (Table 2) by assuming the continuum levels to be the same and tying them together, and we still obtained an acceptable fit, though slightly worse than that given in Table 2; this yielded a much larger value of $N_{\rm H}$ and the covering factor (8.0×10^{23} cm^{-2} and 0.72) at the epoch of orbit 361 than those of orbit 272 (1.9×10^{23} cm^{-2} and 0.29). Both the time-scales of <5 yr and of 5 months are consistent with the motion of gas clouds ($\approx$3400 km s^{-1}) in the BLR for a $\sim 10^7$ M$_\odot$ black hole.

Variable intrinsic emission: For the *ROSAT* low state, the Eddington ratio was estimated conservatively to be $L_{\rm bol}/L_{\rm Edd} <$ several times 10^{-4}, much lower than the critical accretion rate (see Section 1). This value indicates that the accretion proceeded via a RIAF. A RIAF has been postulated to be present in some LLAGN (e.g. Fabian & Rees 1995; Lasota et al. 1996; Quataert et al. 1999; Ptak et al. 2004). In particular, the prototype of such a class, the LINER NGC 4258 (Lasota et al. 1996), has values of $M_{\rm bh}$ and $L_{\rm X}$ similar to those we found for NGC 7589. A thin disc would be truncated and only exist at large radii (e.g. Quataert et al. 1999; Lu & Wang 2000; Meyer & Meyer-Hofmeister 2002). The broad iron line and reflection hump, which are characteristic of typical Seyferts and believed to be evidence for a thin disc, are not expected to be seen in a RIAF. These different accretion modes also predict distinct spectral shapes in the broad-band spectral energy distribution (SED) and possibly in the X-ray spectra. Therefore a good X-ray spectrum and/or SED in a low state is essential to test the RIAF hypothesis.

In the *XMM* high state, the identification of the accretion mode is not clear. The value of $L_{\rm bol}/L_{\rm Edd}$ was estimated to be a few per cent, which is immediately close to the critical value. Thus the accretion flow was possibly in a transition state between a RIAF and a thin disc. Had the flux ever reached a peak much higher than the *XMM* high state sometime between the observations, a transition of the accretion mode might have taken place, according to the current accretion theories. The observed time-scale of $\lesssim$5 yr is consistent with the mass diffusion time-scale on which a thin disc drifted inwards down to several Schwarzschild radii $R_{\rm S}$ from a transition radius of up to $\sim$ hundreds $R_{\rm S}$. However, the quality of the obtained X-ray spectra does not allow us to distinguish between a dominating thin disc (extending down to a few $R_{\rm S}$) and a disc truncated at $\sim$ hundreds $R_{\rm S}$, though the probable spectral flattening – if this is indeed due to reflection of the X-rays – would favour the former. Deep X-ray observations for NGC 7589 and for more objects of this kind are essential for a serious confrontation of current accretion theories.

Large X-ray variability events appear to be rare. The first results from our programme, which searched over 386 *XMM* fields previously covered with *ROSAT* pointed observations, yielded only one, or possibly two, detections. The total sky area covered (66 deg^2) contains, statistically, $\sim$26 galaxies brighter than 15 mag$_B$ and $\sim$180 galaxies brighter than 16.4 mag$_B$ (cf. 15.2 mag$_B$ for NGC 7589). A further extensive search, as well as the measurement of the variability time-scale, is needed in order to be able to estimate the event rate.

ACKNOWLEDGMENTS

We thank Cheng Li and Tinggui Wang for helping with the subtraction of the stellar spectrum, and Christopher Brindle for help in verifying the *XMM* OM results. WY thanks Matteo Guainazzi for useful discussion. Funding for the creation and distribution of the SDSS Archive has been provided by the Alfred P. Sloan Foundation, the Participating Institutions, the National Aeronautics and Space Administration, the National Science Foundation, the US Department of Energy, the Japanese Monbukagakusho, and the Max Planck Society. This research has made use of the NASA/IPAC Extragalactic Database (NED).

REFERENCES

Done, Mulchaey J. S., Mushotzky R. F., Arnaud K. A., 1992, ApJ, 395, 275
Esin A. A., McClintock J. E., Narayan R., 1997, ApJ, 489, 865
Halderson E., Moran E. C., Filippenko A. V., Ho L. C., 2001, ApJ, 122, 637
Fabian A. C., Rees M. J., 1995, MNRAS, 277, L55
Filippenko A., Terlevich R., 1992, ApJ, 379, L79
Fukazawa Y., Iyomoto N., Kubota A., Matsumoto Y., Makishima K., 2001, A&A, 374, 73
Guainazzi M., Marshall W., Parmar A. N., 2001, MNRAS, 323, 75
Heckman T., 1980, A&A 87, 152
Ho L. C., Filippenko A. V., Sargent W. L. W., 1997, ApJ, 487, 568
Ho L. C., Filippenko A. V., Sargent W. L. W., 2003, ApJ, 583, 159
Ho L. C., 2004, in Ho L. C., ed., Carnegie Obser. Astrophys. Ser. Vol. 1, Coevolution of Black Holes and Galaxies. Cambridge Univ. Press, Cambridge, p. 292
Komossa S., Böhringer H., Huchra J., 1999, A&A, 349, 88
Komossa S., Burwitz V., Predehl P., Kaastra J., 2001, in Knapen J. H., Beckman J. E., Shlosman I., Mahoney T. J., eds, ASP Conf. Ser. Vol. 249, The Central kpc of Starbursts and AGN. Astron. Soc. Pac., San Francisco, p. 411
Lasota J.-P. et al., 1996, ApJ, 462, 142
Li C., Wang T.-G., Zhou H.-Y., Dong X.-B., Cheng F.-Z., 2004, AJ, submitted (astro-ph/0407015)
Lu Y., Wang T., 2000, ApJ, 537, L103
Meyer F., Liu B. F., Meyer-Hofmeister E., 2000, A&A, 354, L67
Meyer F., Meyer-Hofmeister E., 2002, A&A, 392, L5
Nandra K., George I. M., Mushotzky R. F., Turner T. J., Yaqoob T., 1997, ApJ, 476, 70
Narayan R., Mahadevan R., Quartaert E., 1998, in Abramowicz M. A. et al., eds, The Theory of Black Hole Accretion Discs. Cambridge Univ. Press, p. 148
Pickering T. E., Impey C. D., van Gorkom J. H., Bothun G. D., 1997, AJ, 114, 1858
Ptak A., Terashima Y., Ho L. C., Quataert E., 2004, ApJ, 606, 173
Ptak A., Mushotzky R., Serlemitsos P., Griffiths R., 1998, ApJ, 501, L37
Quataert E., di Matteo T., Narayan R,, Ho L. C., 1999, ApJ, 525, L89
Quataert E., 2001, in Peterson B. M., Polidan R. S., Pogge R. W., eds, Probing the Physics of Active Galactic Nuclei by Multiwavelength Monitoring. Astron. Soc. Pac., San Francisco, p. 71
Risaliti G., Elvis M., Nicastro F., 2002, ApJ, 571, 234
Shakura N. I., Sunyaev R. A., 1973, A&A, 24, 337
Tanaka Y., 1999, in Mineshige S., Wheeler J. C., eds, Disk Instablities in Close Binary Systems. Universal Academic Press, Kyoto, p. 21
Terashima Y., Iyomoto N., Ho L. C., Ptak A. F., 2002, ApJS, 139, 1
Veilleux S., Osterbrock D. E., 1987, ApJS, 63, 195
Watson M. G. et al., 2001, A&A, 365, L51
York D. G. et al., 2000, AJ, 120, 1579
Yuan W., McMahon R., Komossa St., Watson M., 2002, in Jansen F., ed., New Visions of the X-ray Universe in the XMM-Newton and Chandra Era, in press

This paper has been typeset from a TEX/LATEX file prepared by the author.